Lévy noise induced transition and enhanced stability in a gene regulatory network

Fengyan Wu, Xiaoli Chen, Yayun Zheng, Jinqiao Duan, Jürgen Kurths, and Xiaofan Li

Citation: Chaos **28**, 075510 (2018); doi: 10.1063/1.5025235
View online: https://doi.org/10.1063/1.5025235
View Table of Contents: http://aip.scitation.org/toc/cha/28/7
Published by the American Institute of Physics

Lévy noise induced transition and enhanced stability in a gene regulatory network

Fengyan Wu,[1,2,a)] Xiaoli Chen,[1,b)] Yayun Zheng,[1,3,c)] Jinqiao Duan,[1,4,d)] Jürgen Kurths,[5,e)] and Xiaofan Li[4,f)]
[1]*Center for Mathematical Sciences & School of Mathematics and Statistics, Huazhong University of Science and Technology, Wuhan 430074, China*
[2]*College of Mathematics and Statistics, Chongqing University, Chongqing 401331, China*
[3]*Wuhan National Laboratory for Optoelectronics, Wuhan 430074, China*
[4]*Department of Applied Mathematics, Illinois Institute of Technology, Chicago, Illinois 60616, USA*
[5]*Research Domain on Transdisciplinary Concepts and Methods, Potsdam Institute for Climate Impact Research, PO Box 60 12 03, 14412 Potsdam, Germany and Department of Physics, Humboldt University of Berlin, Newtonstrate 15, 12489 Berlin, Germany*

(Received 08 February 2018; accepted 09 May 2018; published online 18 July 2018)

We investigate a quantitative bistable two-dimensional model (MeKS network) of gene expression dynamics describing the competence development in the *Bacillus subtilis* under the influence of Lévy as well as Brownian motions. To analyze the transitions between the vegetative and the competence regions therein, two dimensionless deterministic quantities, the mean first exit time (MFET) and the first escape probability, are determined from a microscopic perspective, as well as their averaged versions from a macroscopic perspective. The relative contribution factor λ, the ratio of non-Gaussian and Gaussian noise strengths, is adopted to identify an optimum choice in these transitions. Additionally, we use a recent geometric concept, the stochastic basin of attraction (SBA), to exhibit a pictorial comprehension about the influence of the Lévy motion on the basin stability of the competence state. Our main results indicate that (i) the transitions between the vegetative and the competence regions can be induced by the noise intensities, the relative contribution factor λ and the Lévy motion index α; (ii) a higher noise intensity and a larger α with smaller jump magnitude make the MFET shorter, and the MFET as a function of λ exhibits one maximum value, which is a signature of the noise-enhanced stability phenomenon for the vegetative state; (iii) a larger α makes the transition from the vegetative to the adjacent competence region to occur at the highest probability. The Lévy motion index $\alpha_0 \approx 0.5$ (a larger jump magnitude with a lower frequency) is an ideal choice to implement the transition to the non-adjacent competence region; (iv) there is an expansion in SBA when α decreases. *Published by AIP Publishing.* https://doi.org/10.1063/1.5025235

There are often extremely unpredictable jumps and heavy tail distributions with non-Gaussian characteristics in nonlinear dynamical systems, which may induce substantial changes in the system's behaviors. Gene expression is a typical complex system of high interest. To extend previous studies of one-dimensional gene regulatory systems with one positive feedback loop, we here analyze the influence of non-Gaussian noise (Lévy motion) as well as Gaussian noise (Brownian motion) on the transitions between the vegetative and the competence states in a bistable two-dimensional MeKS nonlinear gene regulatory system, which contains a positive as well as a negative feedback loop. We characterize basic features of these transitions with simulations of stochastic tools (mean first exit time and first escape probability) and a geometric tool (stochastic basin of attraction). We find that there is a maximum of mean first exit time vs. the relative contribution factor λ, providing an optimal choice of noise intensity on the stability for the vegetative state. We also present an appropriate choice of the Lévy motion index α to make the transition from the vegetative to the competence region occurring at the highest probability.

I. INTRODUCTION

Random fluctuations are ubiquitous in real life and may affect the fundamental dynamical properties of a system. A number of studies have reviewed that noise has rather counterintuitive and constructive effects on the behavior of a dynamical system. Numerous studies in different fields have demonstrated that noise can play a pivotal role in dynamical systems in biology, physics, geophysics, chemistry, finance, or engineering. This topic has attracted more and more attention in recent years.[1–6] The present contribution is devoted to investigating the influence of a combination of Gaussian and non-Gaussian noises on a gene regulatory network, where the interaction of genes is included in substantial extensions to recent studies.

It is known that messenger RNA (mRNA) and protein molecules are synthesized during the process of transcription and translation, respectively, which constitutes major procedures of gene expression. Bioscientists discovered that key

a) fengyan_wu@hust.edu.cn
b) Author to whom correspondence should be addressed: xlchen@hust.edu.cn
c) yayunzh55@hust.edu.cn
d) duan@iit.edu
e) kurths@pik-potsdam.de
f) lix@iit.edu

transcription and regulatory factors switch between the "on" (the high concentration) and the "off"(the low concentration) state repeatedly, often stochastically, even when cells are maintained in constant conditions. This type of spontaneous dynamic behavior is pervasive, appearing in diverse cell types from microbes to mammalian cells. The initiation of transcription, i.e., the binding of RNA polymerase at the promoter region of DNA, is inherently stochastic in biochemical reactions. Furthermore, the variability in a number of regulatory molecules provides noise sources from the extrinsic environment. Together, the inherent uncertainty in gene expression dynamics and external noisy environment make up the intrinsic and extrinsic noise sources.[7–11] Given that, it is necessary to take into account stochastic fluctuations when considering the dynamics of a gene expression system. It is often assumed that the noise is Gaussian. This arises due to the assumption that the perturbation is the result of a large number of independent interactions of bounded strength. However, this assumption is often not appropriate, in particular when the fluctuations are abrupt pulses or extreme events. Just as Levine *et al.*[12] pointed out, pulsatile dynamics can produce "long-tailed" distributions in static measurements based on flow cytometry and microscopy snapshots. Pulsatile dynamics is emerging as a central, and still largely unexplored area in the cell. Furthermore, non-Gaussian distribution appears in biological systems frequently, such as the mutation of individual population processes[13] and burst-like events in cells.[14] In this situation, it is more appropriate to model the fluctuations by a process with heavy tails and discontinuous sample paths.[5,6,15–17] Lévy motion is an appropriate prototype for non-Gaussian processes with jumps. Therefore, we will study here such a basic gene regulatory network under the influence of Lévy motion.

Most of the *Bacillus subtilis* population is in the vegetative state in which the comK gene expresses the ComK protein at a low level. Under nutrient limitation, only a small fraction of *B. subtilis* transiently differentiates into the competence state in which the ComK protein is at a high level, permitting the cell to take up extracellular DNA and to incorporate it into their own chromosome,[18–21] which is regulated by the MeKS network.[22]

To examine noise-induced transitions between both stable states (vegetative state and competence state), two deterministic quantities, the mean first exit time (MFET) and the first escape probability (FEP) from a microscopic perspective, as well as the average first exit time (AMFET) and the average first escape probability (AFEP) from a macroscopic perspective, are utilized here. The MFET characterizes the residence time of a certain stable state and FEP means the transition probability in two directions (namely from the vegetative state to the competence state and vice versa). They are governed by the differential-integral equations (3) and (6). The microscopic perspective indicates that we analyze the dynamical behavior of a system from a certain point (k, s), but in the macroscopic perspective the entirety dynamical behavior in a domain D is regarded. Note that the values of MFET and FEP are dimensionless parameters, and they are used to characterize the influence of noise on the dynamical system. Here, a more general two-dimensional MeKS model describing the competence development in *B. subtilis* under the influence of Lévy as well as Brownian motion is studied. However, it becomes more challenging but difficult to conduct such a simulation in the two-dimensional model with Lévy motions. We manage to calculate these deterministic quantities by accurate and efficient numerical methods,[15,23–30] instead of Monte-Carlo simulations.

The effects of noise on the model of autoregulatory gene expression involving a single gene have been discussed in Refs. 14 and 31. However, the aforementioned work is only for a single gene activating a positive feedback loop but does not consider interactions with other genes. However, the interplay of different genes is crucial for real genomic systems. Pal *et al.*[9] studied a one-dimensional and a two-dimensional model in gene expression dynamics in *B. subtilis*, which is influenced by Gaussian noise only. They obtained some early signatures of regime shifts in gene expression dynamics for the one-dimensional case, such as critical slowing down (CSD), rising variance, and a ratio of two mean first passage times, while for the two-dimensional model, they did not get as many results as for the one-dimensional case. Süel *et al.*[22] computed a set of excursion trajectories triggered by Gaussian noise for the two-dimensional MeKS model in *B. subtilis*. To the best of our knowledge, so far, little work has been committed to effects of noise on the transitions for the two-dimensional model of the MeKS network in *B. subtilis*. Our main goal is to utilize the knowledge of stochastic dynamics,[6] to gain some deeper insight into effects of various noises on the two-dimensional model of the MeKS network, and in particular, we intend to explore and offer clues on the connection between vegetative growth and competence in the MeKS network.

Furthermore, it has been recently discovered that a disease progression can be divided into a normal state, a predisease state, and a disease state,[32,33] similar to the low vegetative state, the medium concentration state, and the high competence state in our work. Huang[34] pointed out that noise in gene expression takes effect on the choices between the normal and the malignant phenotype during cancer progression. Jia *et al.*[35] investigated the stochastic phenotype switching within the bacterial populations and proposed the importance of the identification of the critical state for early diagnosis of complex diseases. However, they merely considered the influence of Gaussian noise. With our exploration of transitions between two stable states in a gene regulatory system, we hope to provide clues for the prevention and therapy of complex diseases. Here, similar experimental techniques are expected to bring out the noise-induced transitions in gene regulatory system.

The rest of this paper is organized as follows. In Section II, we introduce the two-dimensional deterministic and stochastic MeKS model, and explain concepts about the mean first exit time (MFET), the first escape probability (FEP), and the stochastic basin of attraction (SBA), and present the numerical method for the solutions of MFET and FEP. We show the effects of Lévy motion as well as Brownian motion in the MeKS gene regulatory system in Section III. Finally, some conclusions are summarized in Section IV.

II. MODEL AND METHOD

A. The dynamical model of MeKS network

The core components of the MeKS network are shown in Fig. 1(a): the autoregulatory positive feedback loop regulated by the ComK protein, the ComS protein's competitive interference with the proteolytic degradation of the ComK protein, and the indirect repression of the comS gene by the ComK protein.[22,36,37] The ComK protein can activate its own expression, shaping a positive feedback loop.[38,39] Sinderen[40] proposed that the key transcription factor ComK protein, functioning as a master regulator, can activate the transcription of several genes that is necessary for the competence. When the concentration of the ComK protein is high, the competence develops,[41,42] from which we know that the ComK protein occupies a central position in the competence-signal-transduction network. The relationship between the ComK and the ComS protein is responsible for the formation of a negative feedback loop. Together, the positive and negative feedback loops interacting with each other constitute the MeKS network.

To understand how the MeKS network structure determines the dynamics of competence, Süel *et al.*[22] built a mathematical model (1) constrained by experimental observations. This model can be reduced to a system of two ordinary differential equations incorporating both the direct positive and the ComS-regulated negative feedback loops of ComK:

$$\begin{aligned}\frac{dk}{dt} &= a_k + \frac{b_k k^n}{k_0^n + k^n} - \frac{k}{1+k+s},\\ \frac{ds}{dt} &= \frac{b_s}{1+(k/k_1)^p} - \frac{s}{1+k+s}.\end{aligned} \tag{1}$$

For convenience, we name it as MeKS model and write $f(k,s) = a_k + \frac{b_k k^n}{k_0^n+k^n} - \frac{k}{1+k+s}$, and $g(k,s) = \frac{b_s}{1+(k/k_1)^p} - \frac{s}{1+k+s}$. In the MeKS model, the symbols k and s denote the concentration levels of the ComK and ComS proteins, respectively. The basal and fully activated rates of ComK production are a_k and b_k, respectively. The parameter k_0 represents the concentration of the ComK protein needed for a 50% activation. The cooperativities of ComK auto-activation and ComS repression are indicated by the Hill coefficients n and p, respectively. The ComS protein has the maximum expression rate b_s and the half-maximal rate at $k = k_1$. The ComS protein competitively inhibits the degradation activity of the MecA-ClpP-ClpC complex that targets the ComK protein, which is responsible for the nonlinear degradation terms described at the end of the MeKS model (1).

B. The stochastic dynamical model of competence induction

It was found that stochasticity in gene expression can induce random transitions between both stable steady states, giving rise to binary distributions in the cell population, i.e., two pronounced subpopulations with different protein concentrations appear.[7] Indeed, the influence of noise can cause random perturbations to the stable steady state of a system. Sufficiently strong fluctuations enable the system to escape it, residing in another stable steady state.[9,10] The existence of two major ingredients, the positive feedback loop involved in dynamical system and the additional nonlinearity, contribute to the phenomenon of bistability.[42–44]

According to previous works,[9,12,14,31,45] noise is pervasive in the gene expression events. On occasion, these events show burst-like dynamical behaviors. Furthermore, it has been recently found that the noise intensity and the size of jumps related with the Lévy motion index α can take effects on the concentrations within a cell in gene expression.[14] Thus, Brownian motion and α-stable Lévy motion are suitable to model the noise sources in gene regulatory systems. Here, the α-stable Lévy motion has jumps, which is a special kind of non-Gaussian process defined by stable Lévy random variables. It has a larger jump magnitude with lower jump frequency when α closes to 0, while a smaller jump magnitude with higher jump frequency when $\alpha \in (1,2)$. It is substantially different from Brownian motion whose paths are continuous but almost surely nowhere differentiable. The α-stable Lévy motion's paths are continuous from the right and have left limits (càdlàg) at each time.[5,6] Notice that a càdlàg function can only have a countable number of jumps at most, permitting the system to transit between one stable state and another one which is enclosed in a non-adjacent domain.

To investigate effects of stochastic fluctuations on the transitions between the vegetative and the competence region, our stochastic MeKS model is described as

$$\begin{aligned}\frac{dk}{dt} &= f(k,s) + \sigma_k \dot{B}_t^1 + \varepsilon_k \dot{L}_t^1,\\ \frac{ds}{dt} &= g(k,s) + \sigma_s \dot{B}_t^2 + \varepsilon_s \dot{L}_t^2.\end{aligned} \tag{2}$$

Two kinds of noises, Gaussian and non-Gaussian noises, are incorporated in the MeKS model. The symbols σ_k, σ_s represent the intensities of the Gaussian noise, and $\varepsilon_k, \varepsilon_s$ the intensities of the non-Gaussian noise. The symbols B_t^1 and B_t^2 are two independent Brownian motions, L_t^1 and L_t^2 are two independent α-stable Lévy motions, which is a pure jump process and independent of the Brownian motions. Next, we give three basic deterministic quantities to describe the dynamics of (2) from different viewpoints.

C. The method of three deterministic quantities

1. Mean first exit time (MFET)

The MFET is used to characterize the residence time of a certain stable state, and it is also utilized to describe the stability for a certain stable state of the stochastic MeKS model. First, for a bounded domain D enclosing a certain equilibrium, e.g., the vegetative state, we define the first exit time as $\tau_D(\omega) = \inf\{t \geq 0, X_0 = x,\ X_t \in D^c\}$, where D^c denotes the complement set of D in $\mathbb{R}^2$. Then the mean exit time is denoted as $u(x) \triangleq \mathbb{E}\tau_D(\omega) \geq 0$. It is the mean residence time in a certain domain D before exiting to another regime and is used to our analysis from a microscopic perspective. According to Duan,[6] the MFET $u(k,s)$ in our model can be solved by the following differential-integral equations with the Dirichlet

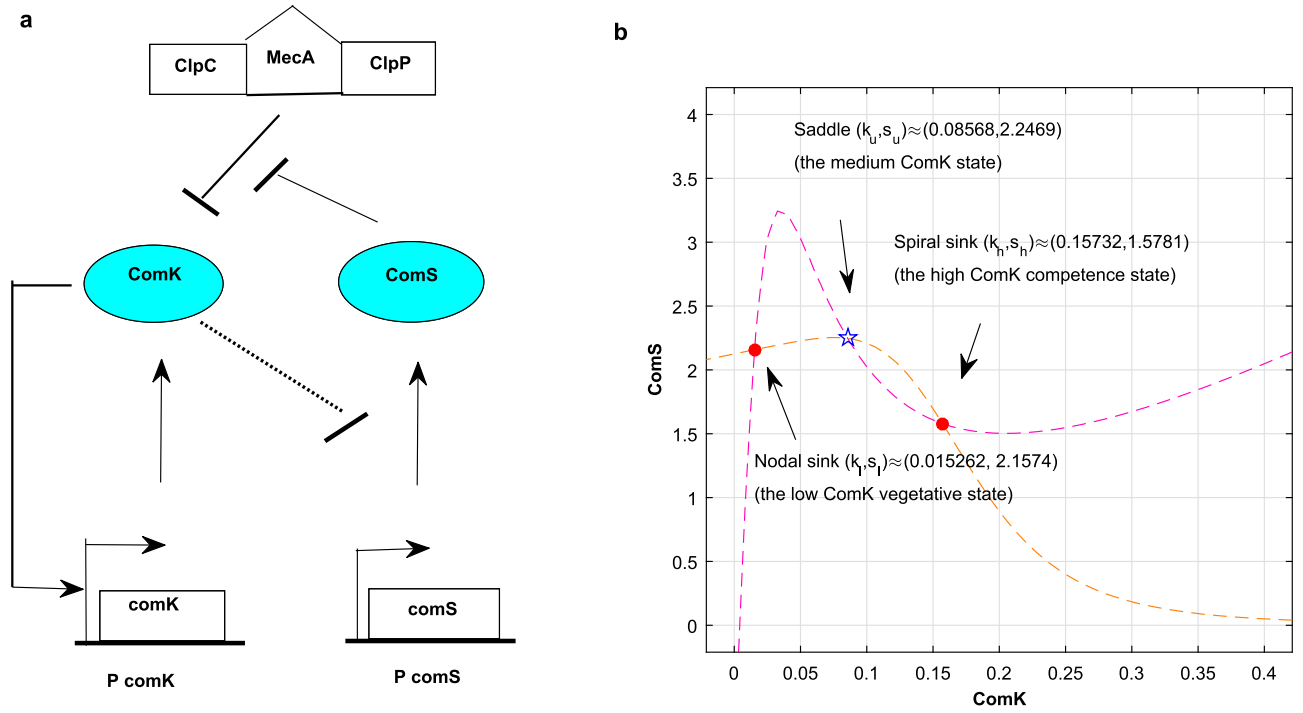

FIG. 1. **The core competence circuit in *B. subtilis* and nullclines for the MeKS model.** (a) $P_{comK}(P_{comS})$ denotes the promoter of gene $comK(comS)$. The arrow signifies the promotion relationship, while the short segment labels the inhibition relationship. ComK protein can active its own expression, forming a positive feedback loop. ComS protein competitively inhibits the degradation activity of the MecA-ClpP-ClpC complex which targets ComK protein, and ComK protein represses the expression of the comS gene indirectly, which are responsible for the negative feedback loop. (b) The intersection points are equilibria corresponding to nodal sink, saddle, and spiral sink.

exterior boundary condition:

$$\begin{aligned} \mathscr{A}u(k,s) &= -1, \quad (k,s) \in D, \\ u(k,s) &= 0, \quad (k,s) \in D^c, \end{aligned} \tag{3}$$

where $D = (a,b) \times (c,d)$ with real numbers a, b, c, d. Here, due to the independent properties of the Brownian and Lévy motion, the jump measure in the two-dimensional case is divided into the summation of two one-dimensional jump measure.[46] Then the generator $\mathscr{A}$ is

$$\begin{aligned} \mathscr{A}u(k,s) = {} & f(k,s)u_k(k,s) + g(k,s)u_s(k,s) + \frac{{\sigma_k}^2}{2}u_{kk} + \frac{{\sigma_s}^2}{2}u_{ss} \\ & + \varepsilon_k^{\alpha} C_\alpha \int_{\mathbb{R}\setminus\{0\}} \frac{u(k+k',s)-u(k,s)}{|k'|^{1+\alpha}} dk' \\ & + \varepsilon_s^{\alpha} C_\alpha \int_{\mathbb{R}\setminus\{0\}} \frac{u(k,s+s')-u(k,s)}{|s'|^{1+\alpha}} ds'. \end{aligned} \tag{4}$$

Secondly, the average mean first exit time (AMFET) on D is defined as $\bar{u}(D) = \frac{1}{|D|}\int\int_D u(k,s)dkds$ for our analysis from a macroscopic perspective.[6,28]

It is worth pointing out that the differential-integral equation (3) is different from the following Fokker-Planck equation:[47]

$$\frac{\partial P}{\partial t} = -\frac{\partial}{\partial x}[f(x,t)P] + Q\int_{-\infty}^{+\infty} \frac{P(z,t)-P(x,t)}{|x-z|^{\alpha+1}} dz. \tag{5}$$

Although they both describe the influence of a non-Gaussian process for a stochastic system, they characterize different aspects. Equation (3) presents the mean first exit time for an orbit starting at a certain interior point of a domain, while Eq. (5) describes the anomalous diffusion in the form of symmetric Lévy flights.[47]

2. First escape probability (FEP)

The escape probability here is employed to characterize the likelihood of the transition between the low vegetative and the high competence region for the MeKS system. The FEP $p(k,s)$ can be solved by the following differential-integral equations with the Balayage-Dirichlet exterior boundary condition:

$$\mathscr{A}p(k,s) = 0, \quad (k,s) \in D, \tag{6}$$

$$p(k,s) = \begin{cases} 1, & (k,s) \in E; \\ 0, & (k,s) \in D^c \setminus E. \end{cases} \tag{7}$$

Here $\mathscr{A}$ is the same generator as in (4).

The average first escape probability (AFEP) on D is defined as $\bar{p}(D) = \frac{1}{|D|}\int\int_D p(k,s)dkds$.[6,28] We use the FEP to examine the transitions from a microscopic viewpoint, and the AFEP from a macroscopic perspective.

3. Stochastic basin of attraction (SBA)

Inspired by Refs. 14, 48, and 49, we would like to use the stochastic basin of attraction (SBA) to make a quantification for the stability of a given competence state (spiral sink) in $\mathbb{R}^2$.

The SBA of an attractor with the open deterministic domain of attraction B is the set $B(u^*,p^*) \triangleq K \cup M$, where $K = \{(k,s) \in B | u(k,s) \geq u^*\}, M = \{(k,s) \in K^c | p(k,s) \geq p^*\}$. $u(k,s)$ is the mean first exit time defined in (3) and $p(k,s)$ is the first escape probability defined in (6).

D. Numerical method

To solve the MFET and the FEP efficiently and accurately, Gao *et al.*[23] constructed an effective numerical method to solve the aforementioned differential-integral equations. They used the central difference for derivatives and a modified trapezoidal rule to discretize the differential-integral equations.[23] Their scheme can be modified for our model with two transformations, i.e., $k = \frac{b-a}{2}z + \frac{b+a}{2}$ for $z \in (-1, 1)$, and $s = \frac{d-c}{2}w + \frac{d+c}{2}$ for $w \in (-1, 1)$, correspondingly, $k' = \frac{b-a}{2}\hat{k}$ and $s' = \frac{d-c}{2}\hat{s}$. We let $v(z, w) = u(\frac{b-a}{2}z + \frac{b+a}{2}, \frac{d-c}{2}w + \frac{d+c}{2})$ and address the integral term in Eq. (4) by the Cauchy principal value integral. Then the generator $\mathscr{A}$ can be rewritten as

$$\begin{aligned}\mathscr{A}v(z,w) = {} & \frac{2}{b-a} f\left(\frac{b-a}{2}z + \frac{b+a}{2}, \frac{d-c}{2}w + \frac{d+c}{2}\right) \\ & \times v_z(z,w) + \frac{4}{(b-a)^2}\frac{\sigma_k^2}{2}v_{zz} \\ & + \frac{2}{d-c} g\left(\frac{b-a}{2}z + \frac{b+a}{2}, \frac{d-c}{2}w + \frac{d+c}{2}\right) \\ & \times v_w(z,w) + \frac{4}{(d-c)^2}\frac{\sigma_s^2}{2}v_{ww} \\ & - \frac{\varepsilon_k^\alpha C_\alpha}{\alpha}\left(\frac{2}{b-a}\right)^\alpha \left[\frac{1}{(1+z)^\alpha} + \frac{1}{(1-z)^\alpha}\right] v(z,w) \\ & - \frac{\varepsilon_s^\alpha C_\alpha}{\alpha}\left(\frac{2}{d-c}\right)^\alpha \left[\frac{1}{(1+w)^\alpha} + \frac{1}{(1-w)^\alpha}\right] v(z,w) \\ & + \varepsilon_k^\alpha C_\alpha \left(\frac{2}{d-c}\right)^\alpha \int_{-1-z}^{1-z} \frac{v(z+\hat{k}, w) - v(z,w)}{|\hat{k}|^{1+\alpha}} d\hat{k} \\ & + \varepsilon_s^\alpha C_\alpha \left(\frac{2}{d-c}\right)^\alpha \int_{-1-w}^{1-w} \\ & \times \frac{v(z, w+\hat{s}) - v(z,w)}{|\hat{s}|^{1+\alpha}} d\hat{s} = \phi(z,w).\end{aligned}$$

Here $\phi(z, w)$ stands for the right-hand side term occurring at the differential-integral equation. For Eq. (3), $\phi(z, w) = -1$. While for Eq. (6), the expression of $\phi(z, w)$ varies with the different escape scenarios. In detail, first, for the adjacent scenario, if the system escapes from region $D = (a, b) \times (c, d)$ to an adjacent region $E = (b, i) \times (c, d)$, then $\phi(z, w) = \frac{\varepsilon_k^\alpha C_\alpha}{\alpha}\{(i - \frac{b-a}{2}z - \frac{b+a}{2})^{-\alpha} - [\frac{b-a}{2}(1-z)]^{-\alpha}\}$, especially, for $i = \infty$, $\phi(z, w) = -\frac{\varepsilon_k^\alpha C_\alpha}{\alpha}(\frac{2}{b-a})^\alpha \frac{1}{(1-z)^\alpha}$. Reversely, if the system escapes from region $D = (a, b) \times (c, d)$ to an adjacent region $E = (h, a) \times (c, d)$, then $\phi(z, w) = \frac{\varepsilon_k^\alpha C_\alpha}{\alpha}\{(\frac{b-a}{2}z + \frac{b+a}{2} - h)^{-\alpha} - [\frac{b-a}{2}(1+z)]^{-\alpha}\}$. Secondly, for the non-adjacent scenario, if the system escapes from region $D = (a, b) \times (c, d)$ to a non-adjacent region $E = (h, i) \times (c, d)$, then $\phi(z, w) = \frac{\varepsilon_k^\alpha C_\alpha}{\alpha}\{(i - \frac{b-a}{2}z - \frac{b+a}{2})^{-\alpha} - (h - \frac{b-a}{2}z - \frac{b+a}{2})^{-\alpha}\}$. Reversely, if the system escapes from region $D = (a, b) \times (c, d)$ to a non-adjacent region $E = (h, i) \times (c, d)$, then $\phi(z, w) = \frac{\varepsilon_k^\alpha C_\alpha}{\alpha}\{(\frac{b-a}{2}z - \frac{b+a}{2} - h)^{-\alpha} - (\frac{b-a}{2}z - \frac{b+a}{2} - i)^{-\alpha}\}$.

III. RESULTS AND DISCUSSION

To illuminate our approach, we choose parameters of the bistability region for our numerical experiments,[22] namely, $a_k = 0.004, b_k = 0.14, b_s = 0.68, k_0 = 0.2, k_1 = 0.222$, $n = 2, p = 5$. With these given parameters, we calculate the nullclines in the ComK-ComS phase plane. It is seen from their nullclines in Fig. 1(b) that there are three equilibria: (i) the nodal sink $(k_l, s_l) \approx (0.015262, 2.1574)$ (the stable vegetative state whose ComK concentration is low), (ii) the saddle $(k_u, s_u) \approx (0.08568, 2.2469)$ (the unstable state whose ComK concentration is medium), and (iii) the spiral sink $(k_h, s_h) \approx (0.15732, 1.5781)$ (the stable competence state whose ComK concentration is high). Next, we present the effects of Gaussian Brownian motion vs. non-Gaussian α-stable Lévy motion on the transition between the low ComK concentration state and the high ComK concentration state (from both microscopic and macroscopic perspectives) as well as basin stability for the competence state in the two-dimensional MeKS model.

Shorter MFET for higher noise intensity and smaller jump magnitude. To consider the residence time of the vegetative stable state, we fix the low vegetative region $D = (0, 0.0793) \times (0, 2.46)$ enclosing the low ComK stable state (k_l, s_l) from the ComK-ComS phase plane. Note that the dimensionless parameter MFET can be relative tiny due to the relative small vegetative region. Now, from microscopic and macroscopic perspectives respectively, we will investigate the influence of Brownian motion and α-stable Lévy motion on the first exit time, which is the mean time of the ComK protein residing in the low vegetative region D before exiting to the high competence region. In Section II, the differential-integral equations (3) offers how to get the mean first exit time $u(k, s)$, which is subject to the nonlocal "Dirichlet" condition, i.e., $u(k, s)$ vanishes outside of D. Appendix presents the numerical method for solving (3).

Without stochastic perturbations, trajectories starting from the initial state around one stable state cannot switch to the region enclosing another stable state. Thus, the residence time staying in the initial region is infinite. However, due to the influence of noise, the system can perform a given transition between both stable states.

Here, we examine the impact of the Brownian motion and α-stable Lévy motion on the mean first exit time, separately. For convenience, we introduce a notation Ψ as the noise intensity under different stochastic fluctuations, i.e.,

$$\begin{cases} \Psi = \varepsilon_k = \varepsilon_s, \sigma_k = \sigma_s = 0. & \alpha \in (0, 2) \\ & (\alpha\text{-stable Lévy motion}), \\ \Psi = \sigma_k = \sigma_s, \varepsilon_k = \varepsilon_s = 0. & \alpha = 2 \ (\textit{Brownian motion}). \end{cases}$$

First, we analyze the noise intensity and Lévy motion index α from a microscopic viewpoint (MFET for the low ComK vegetative state). It is shown in Fig. 2(a) that, when the noise intensity is small enough, MFET increases as α increases, and grows rapidly at $\alpha = 2$ (special case corresponding to Brownian motion). Due to the fact that Brownian motion's trajectories are continuous and cannot jump, the MFET for the Brownian motion is longer than for the Lévy motion. That is, if the noise intensity is slight, then the vegetative state

is more stable under Brownian motion than α-stable Lévy motion. Nonetheless, when the noise intensity becomes larger, the tendency of MFET changes from increase to decrease as α increases, implying that there are critical values of α resulting in a change of MFET from increase to decrease. Meanwhile, when α is fixed at a certain value, there is a decline in MFET as the noise intensity Ψ increases. In other words, Ψ weakens the stability of the vegetative state. The macroscopic situation (AMFET for the low ComK vegetative region) is similar to the consequence in the microscopic situation, we omit its figure here. As shown in Fig. 2(a), a larger Ψ induces a shorter residence time. In addition, compared with Brownian motion, the α-stable Lévy motion makes MFET shorter when Ψ are the same. Together, both microscopic and macroscopic situations demonstrate the consistency of the stability behavior of the state (k_l, s_l).

The pictorial representation of the aforementioned results enlightens us on the transition subject, i.e., if we expect the ComK protein to exit from the low vegetative state to the high competence state, then a higher noise intensity and a larger α (smaller jump magnitude with higher frequency) should be selected.

Optimum choice of noise intensity on the stability of the vegetative state. These results point out different effects of Gaussian noise (Brownian motion) and non-Gaussian noise (α-stable Lévy motion) on the first exit time, individually. Now, we would like to discuss the influence of a combination of both types of noise on the first exit time. Here, we apply the relative contributor factor λ proposed in Ref. 14. In detail, $\lambda = \frac{\varepsilon_k}{\sigma_k}$, where σ_k belongs to $(0, 1]$, ε_k stands for the non-Gaussian noise intensity and σ_k for the Gaussian noise intensity, with the added constraints $\varepsilon_k = \varepsilon_s, \sigma_k = \sigma_s$, and $\varepsilon_k + \sigma_k = 1$.

Figures 2(b) and 2(c) exhibit MFET around the low vegetative state (nodal sink) as a function of λ for $\alpha = 0.5$ and $\alpha = 1.5$, respectively. Note that the total noise intensity is 2 and the vegetative region D is relative small. Thus, the MFET for the region D is not so long, here we focus on the results of MFET vs. λ with various α. From a microscopic viewpoint, we choose four different initial concentrations around the nodal sink, i.e., the red point is in close proximity to the nodal sink, the blue lies in the left direction of the nodal sink, and the green and cyan ones in the right direction of the nodal sink. As shown in Fig. 2(b), with the increase of λ, all initial points of MFET increase fast, after reaching their maxima, the MFET tends to a constant. Meanwhile, the critical point λ_0 corresponding to the maximum of MFET is much larger than 1, implying that the Lévy motion makes a much stronger contribution on MFET than the Brownian one. $\lambda = 0$ is the case where only Brownian motion is considered. Now the noise intensity is 2 and the vegetative region D is small, thus the residence time at the region D is tiny but not 0 [see the inset of Fig. 2(b)]. However, from Fig. 2(c), when $\alpha = 1.5$, the critical point λ_0 shifts towards a much smaller value than for $\alpha = 0.5$, signifying that the Brownian motion takes a more significant effect on the MFET gradually. Note that there is an obvious decline in MFET before arrival at a constant concentration. Furthermore, compared with Figs. 2(b) and 2(c), MFET for $\alpha = 0.5$ is much higher for $\alpha = 1.5$.

Next, we turn to the macroscopic viewpoint. The graphic representation of Fig. 2(d) is more or less the same as that of Fig. 2(b). It is worth noticing that, when λ is fixed, AMFET takes on a rising trend as α decreases, which implies that a smaller α can stabilize the vegetative state. Simultaneously, due to the gradually significant effect on MFET by the Brownian motion, the critical point λ_0 shifts towards a much smaller value as α increases.

Together, the critical point λ_0 corresponding to the maximum of MFET provides the optimum choice of noise intensity on the stability for the vegetative state. When the ratio of both noise intensities equals λ_0, it is more difficult to exit the vegetative region. In other words, noises determined by this ratio can enhance stability of the vegetative state. Actually, this is the phenomenon of noise-enhanced stability, a resonance-like effect, which has been found experimentally and theoretically in various systems.[50–53] However, if we want to weaken the stability of the vegetative state, and expect the concentration of the ComK protein to acquire a high level, then a larger value of α is useful.

First escape probability. Now, we employ another concept to discuss the impacts of the noise intensity and α on the behavior of the transition probability, i.e., the likelihood of the first switching to an escape-target region. Here, we are concerned with the escape probability between the low vegetative region and the high competence region. According to the escaping phenomenon, there are two scenarios of the escape-target region: one is adjacent to the boundary of the starting region, but the other is non-adjacent. Due to the vital role of the ComK protein in the competence development, we just consider the ComK concentration, i.e., the horizontal coordinate of a region is our concern. The first escape probability governed by the differential-integral equations (6) can be solved by a numerical scheme efficiently given in Appendix.

Escape probability from the vegetative region to the adjacent competence region. In this part, we are concerned with the escape probability from the vegetative region $D = (0, 0.0793) \times (0, 2.46)$ to the adjacent competence region $E = (0.0793, \infty) \times (0, 2.46)$. From a microscopic perspective, Figs. 3(a)–3(c) depict FEP as a function of α with different noise intensities. Figure 3(a) describes the behavior of the escape probability of the left point of the nodal sink. As shown in the figure for different noise intensities, as α increases, there is an increasing tendency in FEP initially, but after reaching its maximum, FEP declines slowly. Notice that FEP is smallest at $\alpha = 2$ (Brownian motion), because the trajectories of the Brownian motion cannot jump. From Fig. 3(b), we find that the behavior of the FEP of the point near the nodal sink is similar, except the much slower decline rate. However, for the right point of the nodal sink [Fig. 3(c)], the FEP increases as α increases. Interestingly, due to its relative high concentration, the smallest noise intensity ($\Psi = 0.0125$) makes FEP decreasing at $\alpha = 2$. However, other noise intensities lead FEP to increase. This is because $\Psi = 0.0125$ is so tiny that it could not influence the Brownian motion. But when Ψ becomes bigger, note that the right point of the nodal sink is close to the right boundary of the vegetative region, it is easy to drive the trajectories of Brownian motion to the

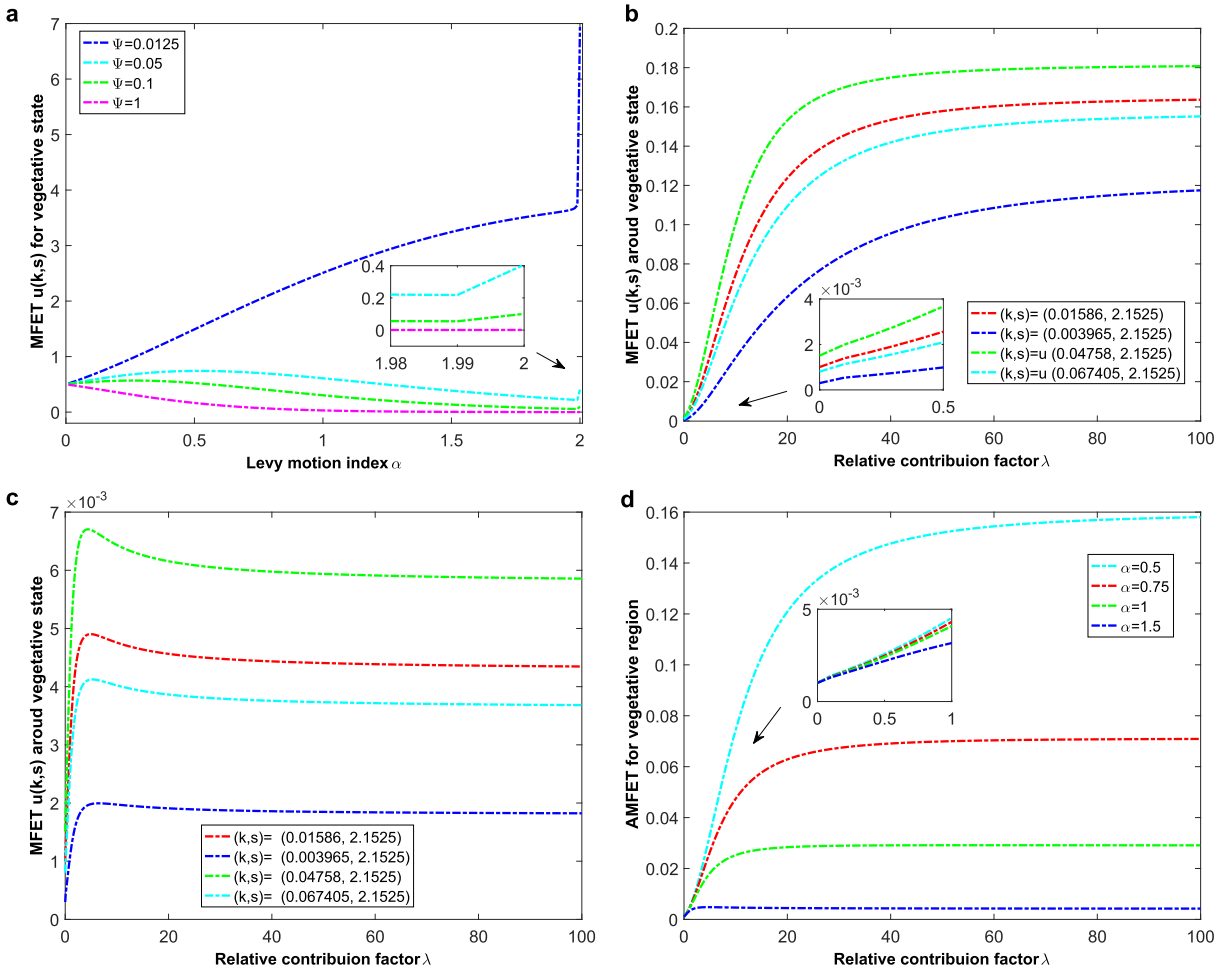

FIG. 2. **Effects of Ψ, α, and λ on the MFET for the low ComK vegetative region.** (a) MFET for the vegetative state (nodal sink) versus α with different noise intensities Ψ. (b) MFET of different initial concentrations versus λ, when $\alpha = 0.5$. (c) MFET of different initial concentrations versus λ, when $\alpha = 1.5$. (d) AMFET versus λ for different α.

adjacent competence region. Compared with Figs. 3(a)–3(c), we observe that the transition probability varies with different initial concentrations, and it increases when the ComK protein initial concentration (k, s) is close to the relative high concentration.

Now, we turn to look at the whole escape behavior. It is shown in Fig. 3(d) that, for the smallest noise intensity ($\Psi = 0.0125$), the escape behavior is about the same as the point near the nodal sink in Fig. 3(b). While for other noise intensities, AFEP increases as α increases, the AFEP drops at $\alpha = 2$ (Brownian motion).

Escape probability from the vegetative region to the non-adjacent competence region. The escape probability from the vegetative region $D = (0, 0.04) \times (1.26, 2.46)$ to the non-adjacent competence region $E = (0.138, 0.178) \times (1.26, 2.46)$ including the spiral sink is considered in this part, and the areas of the two regions are the same. There exists a critical value of α_0 with the highest escape probability in Figs. 3(e) and 3(f). First, from a microscopic perspective, Fig. 3(e) depicts FEP as a function of α with different noise intensities. As α increases, there is an increasing tendency in FEP initially, but after reaching its maximum, FEP drops down to zero. Notice that FEP is much smaller than the adjacent scenario, and it is zero at $\alpha = 2$, due to the fact that Brownian motion's trajectories are continuous, thus they cannot jump. This last result is in accordance with the existing work.[14,54,55] Macroscopically, as shown in Fig. 3(f), the escape behavior of the whole vegetative region enclosing the nodal sink is similar.

Optimum choice for FEP from the vegetative region to the adjacent competence region. To implement the optimum choice for the first escape probability of the transition from the vegetative region $D = (0, 0.0793) \times (0, 2.46)$ to the adjacent competence region $E = (0.0793, \infty) \times (0, 2.46)$, also, the relative contributor factor λ is utilized. Microscopically, in Figs. 4(a) and 4(b), the same four initial concentrations around the low vegetative state (nodal sink) in Figs. 2(b) and 2(c) are selected. As shown in Fig. 4(a), when $\alpha = 0.5$, before entering to their constant concentrations, there is an opposite tendency for different points with the increase of λ, i.e., FEP is decreasing for the two right points of the nodal sink, while the point near the nodal sink and the left point of the nodal sink increase. Meanwhile, the critical value λ_0 corresponding to minima or maxima is large for $\alpha = 0.5$, which indicates that the Lévy motion brings much more contribution to the transition. Then, when $\alpha = 1.5$, there is a similar tendency in Fig. 4(b) with Fig. 4(a), except for the position of the critical value λ_0. Now, macroscopically, in Fig. 4(c),

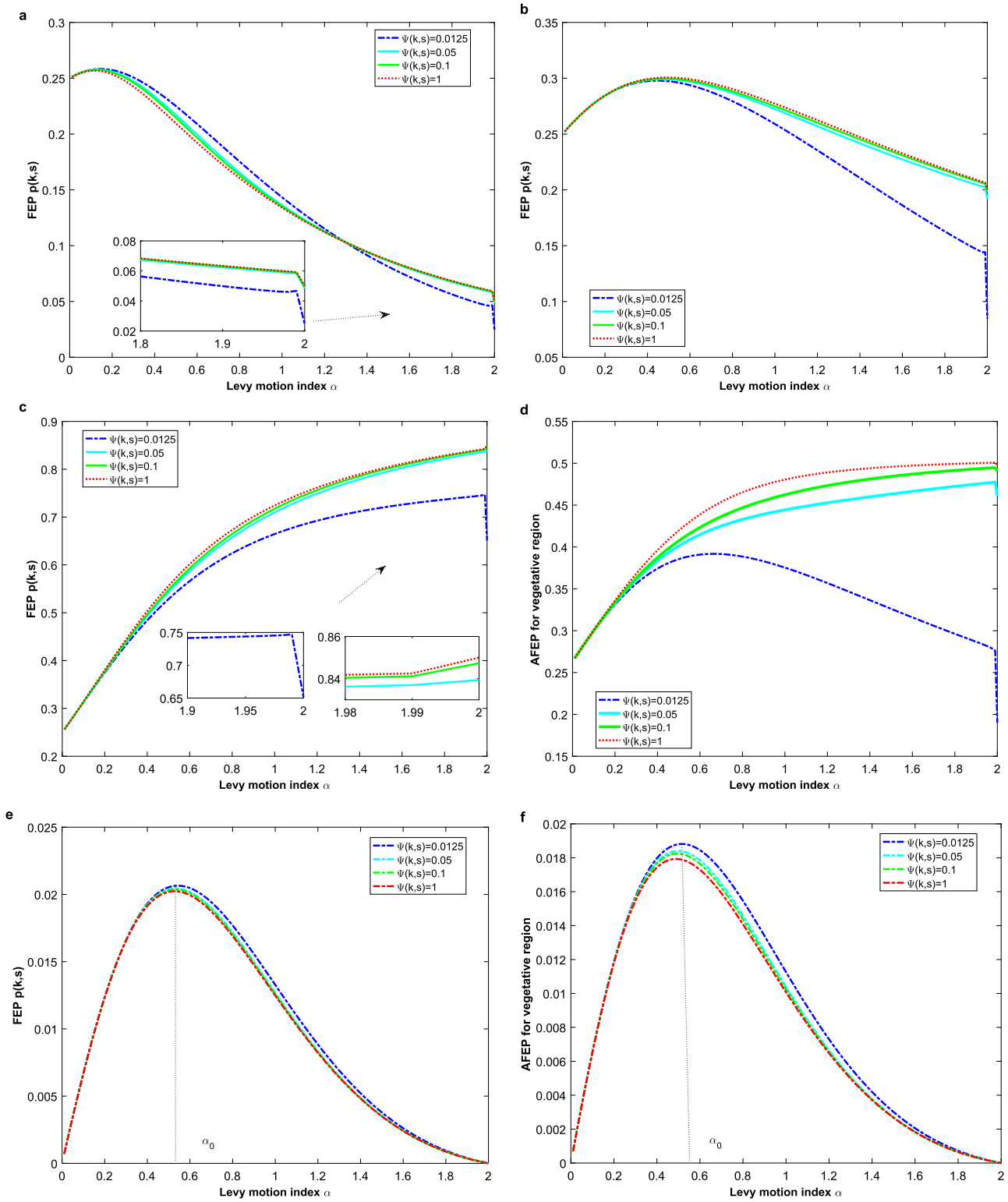

FIG. 3. **Behavior of escape probability from the vegetative region to the competence region for adjacent scenario (a)–(d) and non-adjacent scenario (e) and (f).** (a) Behavior of the FEP for the left point $(0.003965, 2.1525)$ of the vegetative state. (b) Behavior of the FEP for the point $(0.01586, 2.1525)$ is close to the vegetative state [nodal sink $(0.015262, 2.1574)$]. (c) Behavior of the FEP for the right point $(0.067405, 2.1525)$ of the vegetative state. (d) Behavior of the AFEP for the vegetative region. (e) Behavior of the FEP for the vegetative state (nodal sink). (f) Behavior of the AFEP for the vegetative region.

with the increase of λ, a slight increase in AFEP emerges for a much smaller λ, and after reaching its maximum, AFEP declines to arrive at a constant. When λ is fixed at some value, AFEP increases as α increases. This indicates that we can choose a larger α (a smaller jump magnitude with a higher frequency) to make the transition occur at the highest probability.

Optimum choice for FEP from the vegetative region to the non-adjacent competence region. Following up with the optimum choice for the adjacent scenario, the

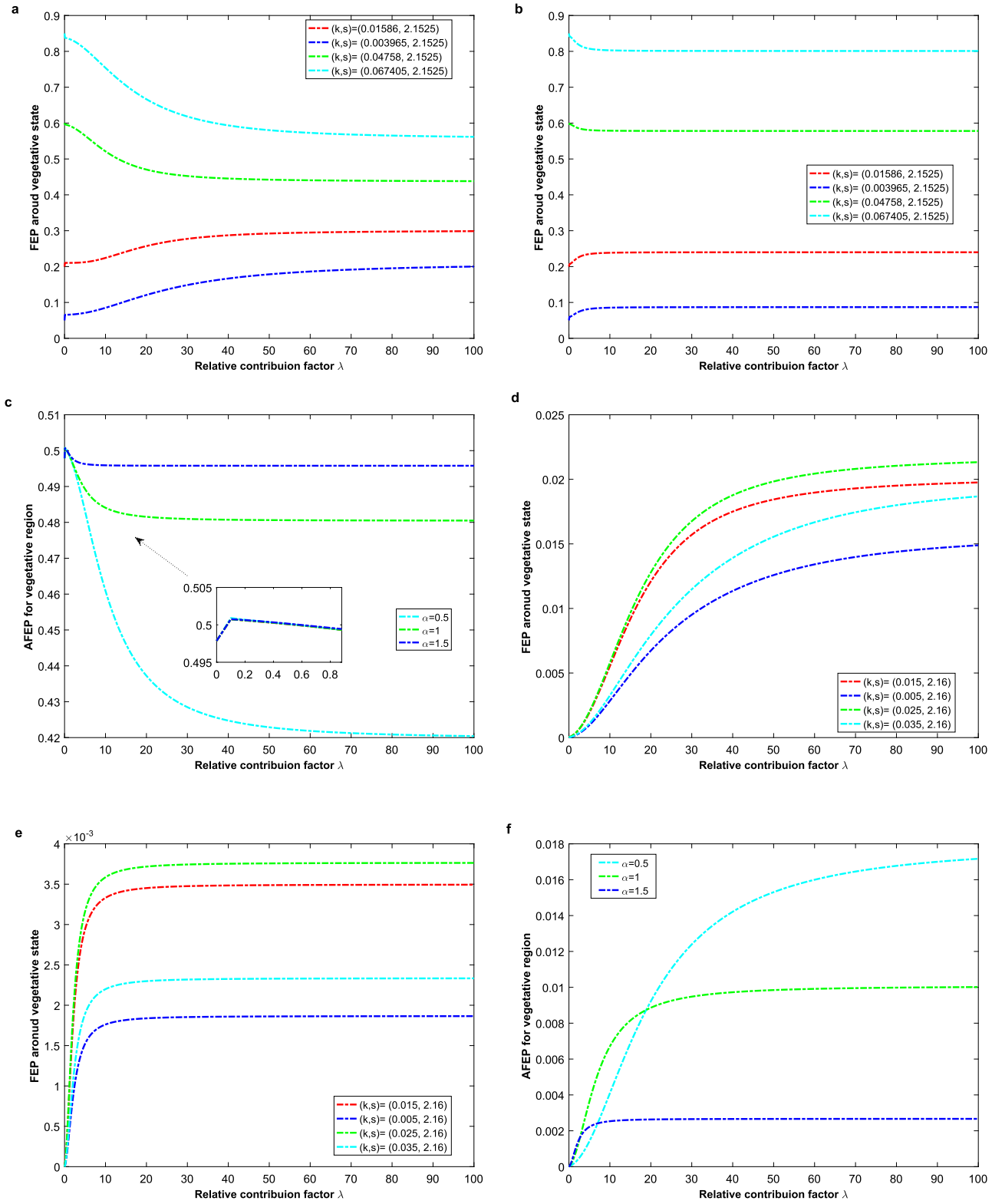

FIG. 4. **Effects of λ on the first escape probability for adjacent senario (a)–(c) and non-adjacent senario (d)–(f)**. (a) FEP of different initial concentrations versus λ, when $\alpha = 0.5$. (b) FEP of different initial concentrations versus λ, when $\alpha = 1.5$. (c) AFEP versus λ with different α. (d) FEP of different initial concentrations versus λ, when $\alpha = 0.5$. (e) FEP of different initial concentrations versus λ, when $\alpha = 1.5$. (f) AFEP versus λ with different α.

relative contributor factor λ is utilized too, for the transition from the vegetative region $D = (0, 0.04) \times (1.26, 2.46)$ to the non-adjacent competence region $E = (0.138, 0.178) \times (1.26, 2.46)$. $\lambda = 0$ means that only Brownian motion is present. Note the fact that the trajectories of Brownian motion are continuous and cannot jump, thus the FEP is 0. Microscopically, four initial concentrations around the low vegetative state (nodal sink) are selected. It is shown in Fig. 4(d) that, when $\alpha = 0.5$, all the selected points increase with the increase of λ. Meanwhile, the critical value λ_0 corresponding

TABLE I. Horizontal coordinate of M ($p^*=0.6, 0.8$) under Lévy motions with different Lévy motion index α.

Noise intensity	α	Horizontal coordinate of M ($p^* = 0.6$)	Horizontal coordinate of M ($p^* = 0.8$)
$\sigma_{k,s} = 1, \varepsilon_{k,s} = 0$	2	$(0.12618, 0.15295) \cup (0.21505, 0.23642)$	$(0.14530, 0.15295) \cup (0.21505, 0.22217)$
$\sigma_{k,s} = \varepsilon_{k,s} = 0.5$	1.5	$(0.11471, 0.15295) \cup (0.21505, 0.25067)$	$(0.13766, 0.15295) \cup (0.21505, 0.22930)$
$\sigma_{k,s} = \varepsilon_{k,s} = 0.5$	0.5	$(0.10324, 0.15295) \cup (0.21505, 0.27916)$	$(0.13001, 0.15295) \cup (0.21505, 0.23642)$

to the maximum is large for $\alpha = 0.5$, implying that the Lévy motion gives much more contribution to the transition. When $\alpha = 1.5$, the tendency in Fig. 4(e) is the same as Fig. 4(d), but the position of the critical value λ_0 shifts towards a much smaller point. Macroscopically, as shown in figure Fig. 4(f), AFEP increases as λ increases. When λ is fixed at a certain value, AFEP increases as α decreases. Hence, the results indicate that $\alpha_0 \approx 0.5$ (a larger jump magnitude with a lower frequency) is an ideal choice to make the transition to a high level at the highest probability.

Larger stochastic basin of attraction (SBA) of competence state for larger jump magnitude. Here, SBA is employed to quantify the stability of a given competence state (spiral sink). We suppose that the total noise intensities are fixed and select the open deterministic domain of attraction $B = (0.115, 0.253) \times (1.06, 3.18)$ enclosing the competence state [spiral sink $(k_h, s_h) \approx (0.15732, 1.5781)$]. We choose $u^* = 0.0038$, and determine $K = (0.15295, 0.21505) \times (1.06, 3.18)$ according to the definition of $K = \{(k, s) \in B \mid u(k, s) \geq u^*\}$. The colorful region is the SBA for the competence state (spiral sink). The yellow area stands for the stochastic invariant set K in which the initial points will stay a longer time. According to $M = \{(k, s) \in K^c \mid p(k, s) \geq p^*\}$, we label the set which has a probability $p^* = 0.6$ return to K with red and green colors, and the probability $p^* = 0.8$ with red color.

Due to the common choice of the criterion $u^* = 0.0038$, we have the same K for the different parameters α. What differentiates the length of the SBA is the second criterion based on the escape probability. In light of the vital role of the ComK protein in the competence development, here, we just consider the ComK concentration, i.e., the horizontal coordinate of SBA is our concern. As shown in Table 1, the horizontal coordinate of M ($p^* = 0.6, 0.8$) expands when α decreases, which implies that the SBA expands when α decreases. Furthermore, Fig. 5 exhibits a pictorial comprehension for the basin stability of the competence state, and there is an expansion in SBA when α decreases. That is, the high competence state is more stable under fluctuations of Brownian motion and α-stable Lévy motion with a smaller α. In other words, Lévy motion with a larger α is more likely to induce a transition to the low vegetative state.

IV. CONCLUSION

In this paper, we have investigated the impacts of stochastic fluctuations on the evolutionary process of a bistable two-dimensional MeKS network system, where (Gaussian) Brownian and (non-Gaussian) α-stable Lévy motion are both incorporated. Two deterministic quantities, the mean first exit time (MFET) and the first escape probability (FEP) from a microscopic perspective as well as the average first exit time (AMFET) and the average first escape probability (AFEP) from a macroscopic perspective, are employed to analyze the transitions between the vegetative and the competence region of the network.

We have found that the noise intensities $\sigma_k, \sigma_s, \varepsilon_k, \varepsilon_s$, the Lévy motion index α (related with the jump magnitude and its frequency) have important and subtle influences on MFET and FEP. We have used the relative contribution factor λ, the ratio between non-Gaussian and Gaussian noise strengths, to identify an optimum choice in the transition between the two states, when the total quantities of the noise intensities are fixed. We here found that MFET as a function of λ shows a maximum, signifying the emergence of the noise-enhanced stability phenomenon for the low vegetative state.

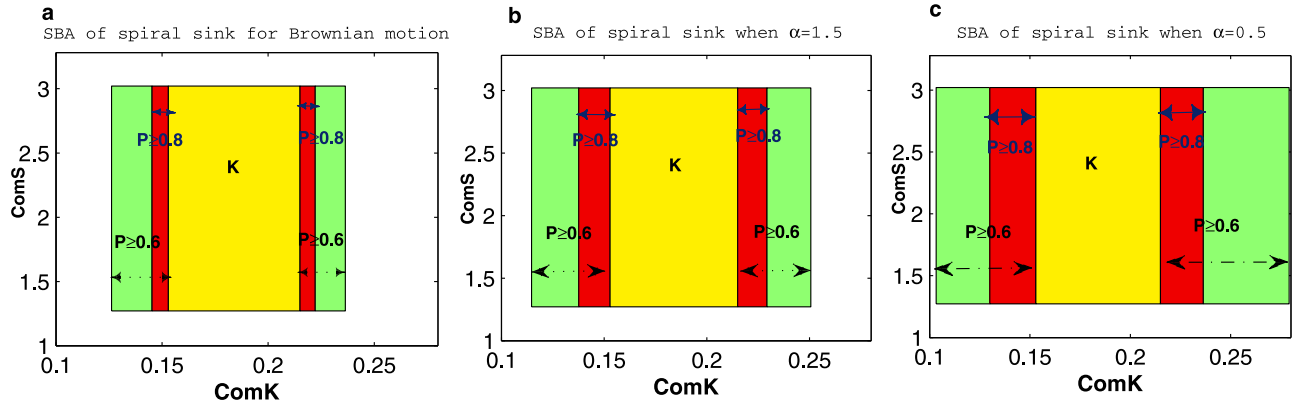

FIG. 5. **Impact of noises on the stochastic basin of attraction (SBA) of the competence state (spiral sink).** (a) SBA for competence state under Brownian motion, $\sigma_k = \sigma_s = 1, \varepsilon_k = \varepsilon_s = 0$. (b) SBA for competence state under α-stable Lévy motion with $\alpha = 1.5$, $\sigma_k = \sigma_s = \varepsilon_k = \varepsilon_s = 0.5$. (c) Same as (b) except $\alpha = 0.5$.

For different initial concentrations, the behavior of the escape probability from the vegetative region to the adjacent competence region is diverse, depending on the influences of the noise intensities and Lévy motion index α. The α-stable Lévy motion can induce a transition between the vegetative region and a non-adjacent competence region, while Brownian motion cannot implement it, due to its continuous paths. Pictorial representations of FEP versus λ indicate that, for the adjacent scenario, a larger α (a smaller jump magnitude with a higher frequency) makes it happen at the highest probability. While for the non-adjacent scenario, $\alpha_0 \approx 0.5$ (a larger jump magnitude with a lower frequency) is the best choice. There exists an ideal choice α_0 for the non-adjacent transition to occur, which is in accordance with Refs. 14, 54 and 55.

Additionally, we have explored the stochastic basin of attraction for the competence state from a geometric viewpoint. Through a schematic presentation of the influence of the Lévy motion index α on the basin stability of the competence region in our stochastic MeKS model, we have detected that the high competence state is more stable under combined fluctuations of Brownian motion and α-stable Lévy motion with a small α.

Theoretically, we have used the knowledge of stochastic dynamics to explore the phenomenon of noise-induced transitions and enhanced stability in a gene regulatory network. Here, we hope that similar experimental techniques would be performed. Furthermore, it has been recently found that a disease progression can be divided into a normal state, a pre-disease state, and a disease state,[32,33] similar to the vegetative state, the medium concentration state, and the competence state in our work. During cancer progression, noise in gene expression takes effects on the choices between the normal and the malignant phenotype.[34] We hope that our exploration will offer a new guidance for the prevention and therapy of complex diseases.

In summary, the highlights of this work are as follows:

- Investigate a bistable two-dimensional genetic network in *B. subtilis*, which includes a positive as well as a negative feedback loop.
- Examine the transitions between the vegetative and competence regimes under non-Gaussian Lévy random fluctuations.
- Characterize some features of noises impact on transitions with simulations of two stochastic tools (mean first exit time and escape probability) and one geometric tool (stochastic basin of attraction).

ACKNOWLEDGMENTS

This work was supported by the National Natural Science Foundation of China (NSFC) (Grant Nos. 11531006, 11371367, and 11271290). We would like to thank Dongfang Li, Xiao Wang, and Hansen Ha for discussions about computation. We are grateful to Aining Bai from the Institute of Botany (Chinese Academy of Sciences), Liang Wang, Mengli Hao, Jian Ren, Tao Jiang, Xinyong Zhang, Yanjie Zhang, and Ziying He for helpful discussions.

APPENDIX: BRIEF INTRODUCTION TO LÉVY MOTION

A Lévy motion L_t is regarded as an appropriate model for non-Gaussian processes with jumps and heavy tails.[56] In detail,

Definition A.1. *A Lévy motion L_t is a stochastic process satisfying*

(i) $L_0 = 0$, *a.s.;*
(ii) Independent increments and stationary increments: for any partition $0 = t_0 < t_1 < \cdots < t_n = t$, *random variables* $L_{t_i} - L_{t_{i-1}} (i = 1 \cdots n)$ *are independent, and for any time* t_1, t_2 *with* $t_1 < t_2$, $L_{t_2} - L_{t_1}$ *and* $L_{t_2 - t_1}$ *have the same distribution;*
(iii) Stochastically continuous sample paths: $L(t) \to L(s)$ *in probability, as* $t \to s (s \geq 0)$.

The sample paths of Lévy motion are continuous from the right and have left limits at every time (càdlàg).[5,6] Lévy motion, as a non-Gaussian stochastic process, is a generalization of Gaussian Brownian motion whose sample paths are continuous in time in the common sense.

In our present work, the α-stable Lévy motion with a triplet $(0, 0, \nu_\alpha)$, i.e., a pure jump motion is considered. The parameter α is called Lévy motion index, or stability index. Especially, it is a Brownian motion when $\alpha = 2$. For $0 < \alpha < 2$, the jump measure in the two-dimensional case is defined as $\nu_\alpha = \frac{C_\alpha dy}{\|y\|^{2+\alpha}}$, where $C_\alpha = \frac{\alpha}{2^{1-\alpha}\pi} \frac{\Gamma(1+\frac{\alpha}{2})}{\Gamma(1-\frac{\alpha}{2})}$. The α-stable Lévy motion has a larger jump magnitude with a lower jump frequency for $0 < \alpha < 1$, while it has a smaller jump magnitude with higher jump frequencies for α closes to 2. More details about Lévy motion can be found in Refs. 5, 6, 56, and 57.

[1] P. Bressloff, *Stochastic Processes in Cell Biology* (Springer, 2014).
[2] N. G. van Kampen, *Stochastic Processes in Physics and Chemistry* (North-Holland, 1992).
[3] C. Gardiner, *Handbook of Stochastic Methods* (Springer, Berlin, 2009).
[4] B. Øksendal, *Stochastic Differential Equations: An Introduction with Applications*, 6th ed. (Springer, 2005).
[5] D. Applebaum, *Lévy Processes and Stochastic Calculus*, 2nd ed. (New York Cambridge University Press, 2009).
[6] J. Duan, *An Introduction to Stochastic Dynamics* (New York Cambridge University Press, 2015).
[7] M. Kærn, T. Elston, W. Blake, and J. Collins, "Stochasticity in gene expression: From theories to phenotypes," Nat. Rev. Genet. **6**, 451–464 (2005).
[8] A. Raj and A. Oudenaarden, "Nature, nurture, or chance: Stochastic gene expression and its consequences," Cell **135**, 216–226 (2009).
[9] M. Pal, A. Pal, S. Ghosh, and I. Bose, "Early signatures of regime shifts in gene expression dynamics," Phys. Biol. **10**, 036010 (2013).
[10] C. Zeng, Q. Han, T. Yang, H. Wang, and Z. Jia, "Noise- and delay-induced regime shifts in an ecological system of vegetation," J. Stat. Mech. **2013**, P10017 (2013).
[11] A. Eldar and M. Elowitz, "Functional roles for noise in genetic circuits," Nature **467**, 167–173 (2010).
[12] J. Levine, Y. Lin, and M. Elowitz, "Functional roles of pulsing in genetic circuits," Science **342**, 1193–1200 (2013).
[13] B. Jourdain, S. Méléard, and W. Woyczynski," Lévy flights in evolutionary ecology," J. Math. Biol. **65**, 677–707 (2012).
[14] Y. Zheng, L. Serdukova, J. Duan, and J. Kurths, "Transitions in a genetic transcriptional regulatory system under Lévy motion," Sci. Rep. **6**, 29274 (2016).
[15] M. Hao, J. Duan, R. Song, and W. Xu, "Asymmetric non-gaussian efficts in a tumor growth model with immunization," Appl. Math. Mod. **38**, 4428–4444 (2104).

[16]R. Dar *et al.*, "Transcriptional burst frequency and burst size are equally modulated across the human genome," Proc. Natl. Acad. Sci. **109**, 17454–17459 (2012).
[17]Y. Zhang *et al.*, "Data assimilation and parameter estimation for a multiscale stochastic system with α-stable Lévy noise," J. Stat. Mech. **2017**, 113401 (2017).
[18]D. Dubnau, "DNA uptake in bacteria," Annu. Rev. Microbiol. **53**, 217–244 (1999).
[19]A. Grossman, "Genetic networks controlling the initiation of sporulation and the development of genetic competence in Bacillus subtilis," Annu. Rev. Genet. **29**, 477–508 (1995).
[20]T. Cagătay, M. Turcotte, M. Elowitz, and G. Süel, "Architecture-dependent noise discriminates functionally analogous differentiation circuits," Cell **139**, 512–522 (2009).
[21]A. Mugler *et al.*, "Noise expands the response range of the bacillus subtilis competence circuit," PLoS Comput. Biol. **12**, 1–12 (2015).
[22]G. Süel, J. Garcia-Ojalvo, L. Liberman, and M. Elowitz, "An excitable gene regulatory circuit induces transient cellular differentiation," Nat. Lett. **440**, 545–550 (2006).
[23]T. Gao, J. Duan, X. Li, and R. Song, "Mean exit time and escape probability for dynamical systems driven by lévy noises," SIAM J. Sci. Comput. **36**, A887–A906 (2014).
[24]H. Chen, J. Duan, X. Li, and C. Zhang, "A computational analysis for mean exit time under non-gaussian lévy noises," Appl. Math. Comput. **218**, 1845–1856 (2011).
[25]X. Wang, J. Duan, X. Li, and Y. Luan, "Numerical methods for the mean exit time and escape probability of two-dimensional stochastic dynamical systems with non-Gaussian noises," Appl. Math. Comput. **258**, 282–295 (2015).
[26]D. Li, C. Zhang, and J. Wen, "A note on compact finite difference method for reaction-diffusion equations with delay," Appl. Math. Model. **39**, 1749–1754 (2015).
[27]D. Li and C. Zhang, "Split Newton iterative algorithm and its application," Appl. Math. Comp. **217**(5), 2260–2265 (2010).
[28]J. Lee, A. Cinar, and J. Duan, "Dynamical behavior of the activator-repressor circuit model under random fluctuations," Commun. Nonlin. Sci. Numer. Simul. **16**, 1978–1985 (2011).
[29]F. Wu, X. Cheng, D. Li, and J. Duan, "A two-level linearized compact ADI scheme for two-dimensional nonlinear reaction-diffusion equations," Comput. Math. Appl. **75**, 2835–2850 (2018).
[30]R. Cai, X. Chen, J. Duan, J. Kurths, and X. Li, "Lévy noise-induced escape in an excitable system," J. Stat. Mech. **2017**, 063503 (2017).
[31]T. Yang *et al.*, "Delay and noise induced regime shift and enhanced stability in gene expression dynamics," J. Stat. Mech. **2014**, P12015 (2014).
[32]D. Kim, O. Rath, W. Kolch, and K. Cho, "A hidden oncogenic positive feedback loop caused by crosstalk between Wnt and ERK pathways," Oncogene **26**, 4571–4579 (2007).
[33]N. Kellershohn and M. Laurent, "Prion diseases: Dynamics of the infection and properties of the bistable transition," Biophys. J. **81**, 2517–2529 (2001).
[34]S. Huang, "Genetic and non-genetic instability in tumor progression: Link between the fitness landscape and the epigenetic landscape of cancer cells," Cancer Metastasis Rev. **32**, 423–448 (2013).
[35]C. Jia, M. Qian, Y. Kang, and D. Jiang, "Modeling stochastic phenotype switching and bet-hedging in bacteria: Stochastic nonlinear dynamics and critical state identification," Quant. Biol. **2**, 110–125 (2014).
[36]K. Turgay, J. Hahn, J. Burghoorn, and D. Dubnau, "Competence in Bacillus subtilis is controlled by regulated proteolysis of a transcription factor," Embo J. **17**, 6730–6738 (1998).
[37]M. Ogura, L. Liu, M. Lacelle, M. Nakano, and P. Zuber, "Mutational analysis of ComS: Evidence for the interaction of ComS and MecA in the regulation of competence development in Bacillus subtilis," Mol. Microbiol. **32**, 799–812 (1999).
[38]H. Maamar and D. Dubnau, "Bistability in the Bacillus subtilis K-state (competence) system requires a positive feedback loop," Mol. Microbiol. **56**, 615–624 (2005).
[39]W. Smits *et al.*, "Stripping Bacillus: ComK auto-stimulation is responsible for the bistable response in competence development," Mol. Microbiol. **56**, 604–614 (2005).
[40]D. Sinderen *et al.*, "comK encodes the competence transcription factor, the key regulatory protein for competence development in Bacillus subtilis," Mol. Microbiol. **15**, 455–462 (1995).
[41]M. Samoilov, G. Price, and A. Arkin, "From fluctuations to phenotypes: The physiology of noise," Sci. Stke **2006**, re17 (2006).
[42]J. Veening, W. Smits, and O. Kuipers, "Bistability, epigenetics, and bet-hedging in bacteria," Ann. Rev. Microbiol. **62**, 193–210 (2008).
[43]J. Pomerening, "Uncovering mechanisms of bistability in biological systems," Curr. Opin. Biotechnol. **19**, 381–388 (2008).
[44]J. Ferrell and W. Xiong, "Bistability in cell signaling: How to make continuous processes discontinuous, and reversible processes irreversible," Chaos **11**, 227–236 (2001).
[45]A. Raj, C. Peskin, D. Tranchina, D. Vargas, and S. Tyagi, "Stochastic *mRNA* synthesis in mammalian cells," Plos Biol. **4**, 1707 (2006).
[46]X. Sun, X. Li, and Y. Zheng, "Governing equations for probability densities of Marcus stochastic differential equations with Lévy noise," Stoch. Dyn. **17**, 1750033 (2017).
[47]A. Dubkov, B. Spagnolo, and V. Uchaikin, "Lévy flight superdiffusion: An introduction," Int. J. Bifurcat. Chaos **18**(9), 2649–2672 (2008).
[48]P. Menck, J. Heitzig, N. Marwan, and J. Kurths, "How basin stability complements the linear-stability paradigm," Nat. Phys. **9**, 89–92 (2014).
[49]L. Serdukova, Y. Zheng, J. Duan, and J. Kurths, "Stochastic basin of attraction for metastable states," Chaos **26**, 1–11 (2016).
[50]I. Dayan, M. Gitterman, and G. Weiss, "Stochastic resonance in transient dynamics," Phys. Rev. A **46**, 757–761 (1992).
[51]R. Mantegna and B. Spagnolo, "Noise enhanced stability in an unstable system," Phys. Rev. Lett. **76**, 563 (1996).
[52]A. Fiasconaro, B. Spagnolo, and S. Boccaletti, "Signatures of noise-enhanced stability in metastable states," Phys. Rev. E **72**, 061110 (2005).
[53]A. Fiasconaro and B. Spagnolo, "Stability measures in metastable states with Gaussian colored noise," Phys. Rev. E **80**, 041110 (2009).
[54]P. Imkeller and I. Pavlyukevich, "Lévy flights: Transitions and meta-stability," J. Phys. A: Math. Gen. **39**, L237–L246 (2006).
[55]P. Imkeller, I. Pavlyukevich, and T. Wetzel, "First exit times for lévy-driven diffusions with exponentially light jumps," Ann. Probab. **37**, 530–564 (2009).
[56]K. Sato, *Lévy Processes and Infinitely Divisible Distributions* (New York Cambridge University Press, 1999).
[57]G. Samorodnitsky and M. Taqqu, *Stable Non-Gaussian Random Processes: Stochastic Models with Infinite Variance* (London Chapman Hall, 1994).